

Benign Overfitting with Quantum Kernels

Joachim Tomasi^{1,2}, Sandrine Anthoine², and Hachem Kadri¹

¹Aix-Marseille University, CNRS, LIS, Marseille, France

²Aix-Marseille University, CNRS, I2M, Marseille, France

{firstname.lastname}@univ-amu.fr

Abstract

Quantum kernels quantify similarity between data points by measuring the inner product between quantum states, computed through quantum circuit measurements. By embedding data into quantum systems, quantum kernel feature maps, that may be classically intractable to compute, could efficiently exploit high-dimensional Hilbert spaces to capture complex patterns. However, designing effective quantum feature maps remains a major challenge. Many quantum kernels, such as the fidelity kernel, suffer from exponential concentration, leading to near-identity kernel matrices that fail to capture meaningful data correlations and lead to overfitting and poor generalization. In this paper, we propose a novel strategy for constructing quantum kernels that achieve good generalization performance, drawing inspiration from benign overfitting in classical machine learning. Our approach introduces the concept of local-global quantum kernels, which combine two complementary components: a local quantum kernel based on measurements of small subsystems and a global quantum kernel derived from full-system measurements. Through numerical experiments, we demonstrate that local-global quantum kernels exhibit benign overfitting, supporting the effectiveness of our approach in enhancing quantum kernel methods.

1 Introduction

Quantum machine learning (QML) has attracted significant attention in recent years [7, 10, 12, 19], particularly as noisy intermediate-scale quantum (NISQ) devices have become increasingly accessible [35]. Variational quantum algorithms (VQAs), which operate under a hybrid quantum-classical paradigm, have received considerable interest due to their potential to achieve a quantum advantage under NISQ constraints [13, 33]. These algorithms utilize parameterized quantum circuits (PQCs) to compute expectation values of quantum observables, which are then processed classically to update circuit parameters and optimize cost functions, enabling PQCs to serve as machine learning models [6, 30].

Quantum kernels, such as quantum fidelity and quantum embedding kernels, offer alternative approaches that align with the constraints of NISQ-compatible hardware [18, 37, 38]. Data are encoded into quantum systems through a parameterized unitary gate that maps classical data into quantum states, i.e., $x \mapsto U(x)|0\rangle = |\phi(x)\rangle$. This mapping, known as quantum feature map, is the basis of the concept of *quantum kernels*: by encoding classical data into quantum feature states, the quantum fidelity kernel function $k(x, z)$ is defined as the inner product $|\langle \phi(x) | \phi(z) \rangle|^2$. This can be regarded as a quantum analog of the kernel trick. All quantum operations in the quantum kernel space remain linear, akin to classical kernel methods that exploit linear separability in kernel feature spaces [18, 38]. The kernel trick enables nonlinear decision boundaries in the original data space while avoiding explicit computation of high-dimensional features.

While VQAs optimize explicit parameterized models, quantum kernels act as their implicit counterparts, leveraging the inner products of embedded quantum states. This duality establishes a theoretical bridge between certain VQA architectures and kernel-based methods [19, 20, 37]. Quantum kernel methods are founded on the potential to achieve a computational quantum advantage in feature representations [29]. In this paradigm, certain quantum feature maps are proposed to encode data into high-dimensional Hilbert spaces that are classically intractable but remain efficiently computable on quantum hardware [18, 22, 26, 38]. For example, as shown in [26], specific quantum circuits can generate feature maps with provable classical intractability under complexity-theoretic assumptions, potentially enabling learning tasks that are beyond the reach of conventional classical methods. Furthermore, recent work has shown quantum embedding kernels can approximate general classes of functions [15].

However, despite their computational promise, it remains unclear whether quantum advantages in quantum kernels directly translate into practical improvements in learning performance. One concern is that quantum-enhanced features do not necessarily capture the intrinsic structure of the target learning problems. While these quantum models exhibit high expressivity, they often give rise to challenges such as the exponential concentration of kernel values near zero, resulting in kernel matrices that closely approximate the identity matrix [41]. Such behavior undermines the model’s ability to capture meaningful data correlations, ultimately limiting its generalization capability.

To achieve generalization, particularly in the context of quantum kernels, some research has focused on mitigating overfitting through regularization techniques that avoid mere training set interpolation. For example, methods for tuning kernel bandwidths in quantum kernels and reducing the dimensionality of the quantum feature space have been proposed [9, 19, 22, 39]. Inspired by classical approaches in which overparameterized models have strong generalization while achieving near-zero training errors, we are interested in enabling generalization in quantum kernel machines, even in the scenarios where the training set is interpolated. Very few studies have examined the generalization abilities of overparameterized quantum models [14]. [23] has investigated the generalization of overparameterized Quantum Neural Networks (QNNs), while [21] has studied double descent phenomenon in least-squared linear regression within quantum features. [34] has examined benign overfitting in linear quantum models for uniformly spaced training data. In our work, we advance this line of research by proposing a framework for quantum kernels that inherently promotes *benign overfitting*. Drawing on the concept of spiky-smooth kernels [16], we propose a *Local-Global* quantum kernel constructed as a weighted sum of two quantum kernels. One component is derived from a local measurement (i.e., low-dimensional relative to the full quantum embedding space) that mimics the smooth kernel behavior, while the other comes from a global measurement of the entire quantum feature space, capturing the spiky component. This Local-Global quantum kernel leads to good generalization while still interpolating training data, leading to benign overfitting in quantum machine learning.

2 Background

We begin by reviewing benign overfitting in classical kernel regression and quantum kernels, the concepts that form the building blocks of our framework.

2.1 Benign Overfitting in Kernel Regression

Kernel regression Kernel Regression (KR) extends linear ridge regression by mapping input data $\mathbf{x} \in \mathcal{X}$ into a high-dimensional Hilbert space \mathcal{H} via a feature map $\phi : \mathcal{X} \rightarrow \mathcal{H}$. The associated Reproducing Kernel Hilbert Space (RKHS) \mathcal{H}_k is defined through a positive definite kernel k defined as $k(\mathbf{x}, \mathbf{x}') = \langle \phi(\mathbf{x}), \phi(\mathbf{x}') \rangle_{\mathcal{H}}$.

Given a dataset $D_n = \{(\mathbf{x}_i, y_i)\}_{i=1}^n \subset (\mathcal{X} \times \mathbb{R})^n \subset (\mathbb{R}^d \times \mathbb{R})^n$, KR aims to minimize the

empirical risk

$$\mathcal{L}(f, D_n) := \frac{1}{n} \sum_{i=1}^n (y_i - f(x_i))^2, \quad (1)$$

over $f \in \mathcal{H}_k$. The representer theorem guarantees that the solution can be expressed as $f_\alpha(x) = \sum_{i=1}^n \alpha_i k(x_i, x)$, with the coefficient vector α^* obtained by

$$\alpha^* = K^+ \mathbf{y}, \quad (2)$$

where $K \in \mathbb{R}^{n \times n}$ is the kernel matrix with entries $K_{ij} = k(\mathbf{x}_i, \mathbf{x}_j)$ and K^+ denotes the pseudo-inverse of K . When $\dim(\mathcal{H}) = p > n$ this formulation leverages the kernel trick and the representer theorem to transform an overparameterized linear regression problem on \mathcal{H} into a linear regression problem on \mathbb{R}^n [36].

From generalization of overparametrized models to benign overfitting in kernel regression Overparameterized neural networks can demonstrate strong generalization capabilities, even when they nearly interpolate training data, challenging the classical bias-variance tradeoff. This observation has prompted a reevaluation of generalization in modern machine learning [43], leading to various interpretations of the phenomenon. One such interpretation is benign overfitting, or harmless interpolation, where models can overfit the training data without compromising their ability to generalize [1, 31]. In this context, *overfitting* refers to a model trained to (nearly) interpolate the training data, while the terms *benign* or *harmless* describe scenarios in which this overfitting does not negatively impact the model’s generalization ability.

Motivated by the desire to understand this behavior in deep networks, early works explored benign overfitting in simpler models. Notably, [1, 17] studied benign overfitting in overparameterized linear regression, demonstrating that this phenomenon is not limited to deep networks. Furthermore, [27] refined the classification of overfitting by distinguishing between benign, tempered, and catastrophic regimes, which are based on the behavior of the expected risk of interpolating predictors. This phenomenon has also been observed in kernel regression [5, 25], which can be seen as overparameterized linear regression in feature spaces. When the input (or feature) dimension increases with the number of data points, the effective dimension of the kernel matrix grows, and its eigenvalues decay slowly enough that noise gets spread across many less important directions [1, 2, 17, 42]. In this context, the minimum-norm interpolant—i.e., the ridgeless regression solution that minimizes its norm—can memorize noise in redundant directions while still capturing the underlying signal. This behavior has been rigorously characterized in linear regression and extended to kernel methods [27, 42, 44]. In fixed-dimensional settings, some studies showed that benign overfitting can occur under specific conditions, such as constraints on the kernel’s eigenvalue spectrum [3, 11, 27] or on the minimum-norm interpolant [16].

Intuition Benign overfitting in both linear and kernel regression can be understood through a ‘*simple-plus-spiky*’ decomposition of the minimum-norm interpolant [2]. In this decomposition, the ‘*simple*’ component captures the main signal in the data, while the ‘*spiky*’ component locally interpolates noise without significantly affecting overall prediction performance.

Consider the linear model $y_i = \langle \theta^*, \mathbf{x}_i \rangle + \epsilon_i$, where θ^* is the vector of parameters and ϵ_i is the noise. In the overparameterized regime ($d > n$), the minimum-norm interpolant is given by $\hat{\theta} = X^\top (XX^\top)^+ y$, where X is the data matrix. We can always choose a $l \in \mathbb{N}$ to split the features and parameters as $\mathbf{x} = [\mathbf{x}_{\leq l}, \mathbf{x}_{> l}]$ and $\hat{\theta} = [\hat{\theta}_{\leq l}, \hat{\theta}_{> l}]$, so that the prediction function and the covariance matrix decomposes into

$$\hat{f}(\mathbf{x}) = \langle \hat{\theta}_{\leq l}, \mathbf{x}_{\leq l} \rangle + \langle \hat{\theta}_{> l}, \mathbf{x}_{> l} \rangle \quad \text{and} \quad XX^\top = X_{\leq l} X_{\leq l}^\top + X_{> l} X_{> l}^\top.$$

If the term $X_{> l} X_{> l}^\top$ has a sufficiently flat spectrum for some l , we can approximate it by ρI_n , so that $XX^\top \approx X_{\leq l} X_{\leq l}^\top + \rho I$. Under this approximation, the estimator for the first l components

resembles the ridge regression solution

$$\hat{\theta}_{\leq l} \approx \arg \min_{\theta \in \mathbb{R}^l} \|X_{\leq l}\theta - y\|_2^2 + \rho \|\theta\|_2^2.$$

Here, the simple component, $\hat{\theta}_{\leq l}$, captures the primary signal, while the spiky component, $\langle \hat{\theta}_{> l}, \mathbf{x}_{> l} \rangle$, accounts for the interpolation of residual noise.

A similar decomposition applies to kernel regression. The kernel matrix can be expressed as $K = K_{< l} + K_{\geq l} \approx K_{< l} + \rho I$, effectively separating the RKHS-based minimum-norm interpolant into two parts: a regularized component that approximates the underlying signal and a spiky component that locally interpolates noise [24, 25, 27, 28]. In fixed-dimensional settings, where the minimum-norm estimator is known to be inconsistent [4, 8], [16] proposed a prediction rule based on a spiky-smooth kernel of the form $k_{\rho, \gamma}(x, z) = \tilde{k}(x, z) + \rho \hat{k}_\gamma(x, z)$, where \tilde{k} is a smooth universal kernel and \hat{k}_γ is a spiky kernel, enabling benign overfitting.

2.2 Quantum Kernels

Notation According to the bra-ket notation adopted in quantum computing, column vectors are denoted as a 'ket', $|\cdot\rangle$, while row vectors are represented as a 'bra', $\langle \cdot|$. These two are dual to each other, with the bra defined as $\langle \cdot| := |\cdot\rangle^\dagger$, where \dagger denotes the adjoint (or conjugate transpose). The inner product of two states ψ and ϕ is written as $\langle \psi|\phi\rangle$, and their tensor product is denoted either as $|\psi\phi\rangle$, $|\psi\rangle|\phi\rangle$, or equivalently as $|\psi\rangle \otimes |\phi\rangle$. Also, the t -fold tensor product of a state $|\psi\rangle$, denoted by $\bigotimes_{i=1}^t |\psi\rangle$, can be compactly expressed as $|\psi\rangle^{\otimes t}$ or $|\psi^t\rangle$. Quantum states can also be represented using density matrices.

For a pure state $|\psi\rangle$, the density matrix is defined as $\rho = |\psi\rangle\langle\psi|$. In the computational basis, each basis state $|i\rangle$ for $i \in \{0, 1, \dots, 2^n - 1\}$ corresponds to the tensor product of individual qubit states derived from the bit decomposition of i . Quantum observables are represented by Hermitian operators, and the expectation value of an observable O in the state ρ is given by $\langle O \rangle_\rho = \text{Tr}(\rho O)$. For clarity, the subscript ρ is often omitted when the context is clear. Quantum circuits provide a diagrammatic representation of quantum computations. They consist of a sequence of quantum gates—unitary operations applied to qubits—followed by measurements of quantum observables. These circuits offer a structured framework for manipulating quantum states and designing quantum algorithms. For a comprehensive introduction to quantum computing and quantum circuits, readers may refer to [32].

Quantum Encoding and Quantum Kernels A quantum machine learning algorithm needs data in the form of quantum states. So classical data should be first encoded into quantum states, i.e., the transformation of a classical data x to a quantum state $|\phi_x\rangle$. Most of the interest in quantum kernels comes from the observation that encoding classical data into a quantum computer defines an explicit feature representation of the data.

Consider a quantum feature map that encodes a data point x into a quantum state represented by the density matrix ρ_x . A quantum kernel $k(x, z)$ is defined as the Hilbert-Schmidt inner product between the states ρ_x and ρ_z , given by

$$k(x, z) = \text{Tr}[\rho_x \rho_z]. \quad (3)$$

When the data x is encoded into a pure quantum state of the form

$$x \mapsto \rho_x = |\phi_x\rangle\langle\phi_x| = U(x)|0^t\rangle\langle 0^t|U^\dagger(x),$$

the quantum kernel in (3) simplifies to

$$k(x, z) = |\langle\phi_x|\phi_z\rangle|^2 = |\langle 0^t|U^\dagger(z)U(x)|0^t\rangle|^2. \quad (4)$$

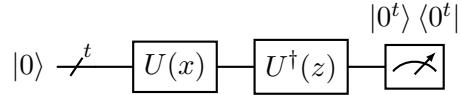


Figure 1: Quantum fidelity kernel. When the input qubit register, here consisting of t qubits, is initialized in $|0^t\rangle$, i.e., all the qubits in the register are initialized in $|0\rangle$, the circuit prepares the quantum state $U^\dagger(z)U(x)|0^t\rangle$. The result of measuring the observable $|0^t\rangle\langle 0^t|$ determines the kernel value, given by $k(x, z) = |\langle \phi_x | \phi_z \rangle|^2 = |\langle 0^t | U^\dagger(z)U(x) | 0^t \rangle|^2$.

This corresponds to measuring the fidelity between the quantum states $|\phi_x\rangle$ and $|\phi_z\rangle$, making this kernel known as the quantum fidelity kernel [29, 38] (see Fig. 1).

Recent studies analyzed generalization error bounds for learning with quantum fidelity kernels and the results appear to be negative [19, 22]. The expressive power of quantum models can hinder generalization. Finding suitable quantum kernels is not easy because the kernel evaluation might require exponentially many measurements. In other words, when using a large number of qubits, the kernel matrix (i.e., the matrix obtained by evaluating the kernel function on all pairs of data points) gets close to the identity matrix, resulting in overfitting and poor generalization performance [40].

To address this issue, [9] introduced bandwidth to quantum fidelity kernels. None of these studies considered new phenomena in modern machine learning, such as benign overfitting. In the following, we show how benign overfitting could change our view of generalization with quantum kernels.

3 Benign Overfitting with Local-Global Quantum Kernel

In the previous section, we described existing quantum kernel techniques. In this section, we present novel contributions that extend the existing literature. We design a new framework taking into consideration the benign overfitting phenomenon to build quantum kernels that can achieve good generalization. Our framework is based on the notion of *local-global* quantum kernel, which can be viewed as a quantum analog of the classical spiky-smooth kernel [16].

3.1 Local-Global Quantum Kernel

Definition 1 (Local-Global Quantum Kernel). Let $U(x)$ be a unitary operator acting on t qubits. Define the local and global quantum states by

$$\rho_x^L = U(x) \left(L_s \otimes \frac{1}{2^{t-s}} I_{t-s} \right) U^\dagger(x), \quad \rho_x^G = U(x) G_t U^\dagger(x),$$

where L_s is a pure quantum state, i.e., a rank-one projector, of $s < t$ qubits and G_t is a pure quantum state of t qubits. The corresponding local and global quantum kernels are defined as $k_L(x, z) = \text{Tr}[\rho_x^L \rho_z^L]$ and $k_G(x, z) = \text{Tr}[\rho_x^G \rho_z^G]$, respectively. The local-global quantum kernel is given by the weighted sum

$$k_{LG}(x, z) = \lambda_L k_L(x, z) + \lambda_G k_G(x, z), \quad (5)$$

where λ_L and λ_G are scalar weights.

The term 'local-global' conveys the intuition that L_s acts as a local projector, whereas G_t serves as a global projector. Specifically, the local kernel is derived from a measurement of a subset of s qubits within the quantum circuit, while the global kernel is obtained through a measurement of overall t qubits. More formally, let us define

$$\sigma_{x,z} := U^\dagger(z)U(x) \left(L_s \otimes \frac{1}{2^{t-s}} I_{t-s} \right) U^\dagger(x)U(z). \quad (6)$$

The local kernel writes as:

$$k_L(x, z) = \text{Tr}[\rho_x^L \rho_z^L] = \frac{1}{2^{t-s}} \text{Tr}[\sigma_{x,z}(L_s \otimes I_{t-s})] = \frac{1}{2^{t-s}} \text{Tr}[\tilde{\sigma}_{x,z} L_s], \quad (7)$$

where $\tilde{\sigma}_{x,z}$ is the partial trace over qubits $s+1$ to t , i.e., $\tilde{\sigma}_{x,z} = \text{Tr}_{s+1:t}[\sigma_{x,z}]$ [22]. As shown in (7), the local kernel corresponds to a measurement performed on a subsystem of $\sigma_{x,z}$. Specifically, if $L_s = |0^s\rangle\langle 0^s|$, then $k_L(x, z)$ measures the probability of locally projecting the first s qubits $\sigma_{x,z}$ onto $|0^s\rangle\langle 0^s|$. On the other hand, G_t is a pure quantum state that can be represented by a rank-one projector, i.e., $G_t = |\psi\rangle\langle\psi| = U_G |0^t\rangle\langle 0^t| U_G^\dagger$, for some unitary operator U_G . Consequently, the kernel k_G is precisely the fidelity kernel defined in (4), which involves a measurement of overall t qubits of the quantum feature space, hence the term global kernel.

The key intuition behind our construction is that as t increases, the kernel matrix generated by the global kernel k_G should tend to the identity matrix. This follows from the fact that inner products between quantum states are expected to vanish as the number of qubits grows [19,22]. In contrast, the local kernel k_L , derived from a local measurement, is expected to yield a smoother kernel matrix with more prominent off-diagonal elements. Following the idea of spiky-smooth kernels [16], the local-global quantum kernel is designed to capture the main signal through its local component while enabling localized noise interpolation via its global part, thereby leading to benign overfitting.

3.2 Separable Global Encoding

To simplify the analysis, we assume that both the global projector G_t and the encoding unitary $U(x)$ admit a separable factorization into q -fold of s -qubits:

$$G_t = L_s^{\otimes q}, \quad U(x) = V_s(x)^{\otimes q}, \quad t = qs,$$

where each $V_s(x)$ acts on s qubits. We call this scheme *Separable Global Encoding*. In this setting, the reduced density matrix of ρ_x^L defined in Definition 1 writes as

$$\tilde{\rho}_x^L := \text{Tr}_{s+1:t}[\rho_x^L] = V_s(x) L_s V_s^\dagger(x).$$

The local kernel is then expressed as

$$\begin{aligned} k_L(x, z) &:= \text{Tr}[\rho_x^L \rho_z^L] = \text{Tr}[(\tilde{\rho}_x^L \otimes \frac{1}{2^{t-s}} I_{t-s})(\tilde{\rho}_z^L \otimes \frac{1}{2^{t-s}} I_{t-s})] \\ &= \frac{1}{2^{(t-s)}} \text{Tr}[\tilde{\rho}_x^L \tilde{\rho}_z^L], \end{aligned}$$

and the global kernel is given by

$$\begin{aligned} k_G(x, z) &:= \text{Tr}[\rho_x^G \rho_z^G] = \text{Tr}[(V_s(x) L_s V_s^\dagger(x) V_s(z) L_s V_s^\dagger(z))^{\otimes q}] \\ &= \text{Tr}[V_s(x) L_s V_s^\dagger(x) V_s(z) L_s V_s^\dagger(z)]^q \\ &= \text{Tr}[\tilde{\rho}_x^L \tilde{\rho}_z^L]^q. \end{aligned}$$

Thus, the local-global kernel reduces to

$$k_{LG}(x, z) = \tilde{\lambda}_L k(x, z) + \lambda_G k(x, z)^q, \quad (8)$$

where $k(x, z) = \text{Tr}[\tilde{\rho}_x^L \tilde{\rho}_z^L]$ and $\tilde{\lambda}_L = \frac{\lambda_L}{2^{t-s}}$.

The local-global quantum kernel includes a parameter q , which determines the kernel's degree and serves as a tuning parameter for controlling the bandwidth of the global component. Figure 2 illustrates this idea. The local-global kernel closely follows the local component but deviates in specific narrow regions. As the parameter q increases, these deviations become more localized, reinforcing the analogy with spiky-smooth kernels.

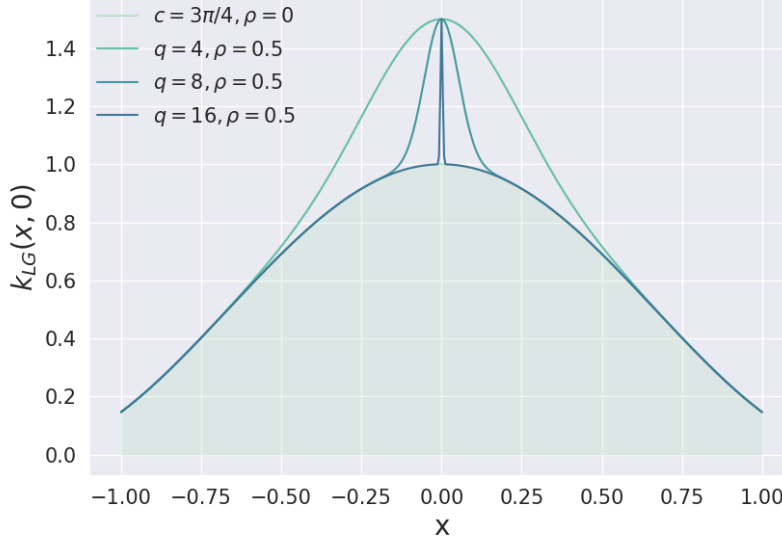


Figure 2: Local-global kernels for with $k_{LG}(x, z) = \cos^2(\frac{c(x-z)}{2}) + \rho \cos^{2q}(\frac{c(x-z)}{2})$, where $c = \frac{3\pi}{4}$, $\rho = 0.5$ and $q = 4, 8, 16$. As we will see in Section 4, the kernel $k(x, z) = \cos^2(\frac{c(x-z)}{2})$ is the fidelity quantum kernel obtained by angle quantum encoding [9].

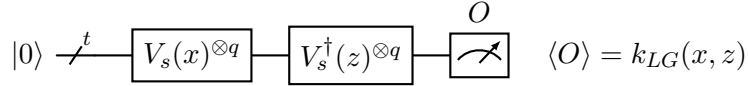


Figure 3: A quantum circuit for computing the local-global kernel k_{LG} using (9) and (10). The measurement operator O is defined as $O = \tilde{\lambda}_L O_L + \lambda_G O_G$, where $O_L = |0^s\rangle \langle 0^s| \otimes I_s^{\otimes q-1}$ and $O_G = (|0^s\rangle \langle 0^s|)^{\otimes q}$.

3.3 Quantum Circuit Implementation

We now turn our attention to the circuit implementation of the local-global quantum kernel. Since it combines a local quantum kernel with a global one, a natural approach to evaluating the local-global kernel is to measure a quantum observable that can be expressed as a weighted sum of local and global observables.

In the case of separable global encoding with $L_s = |0^s\rangle \langle 0^s|$, the reduced density matrix of $\sigma_{x,z}$ defined in (6) is given by:

$$\tilde{\sigma}_{x,z} := \text{Tr}_{s+1:t}[\sigma_{x,z}] = V_s^\dagger(z)V_s(x) |0^s\rangle \langle 0^s| V_s^\dagger(x)V_s(z). \quad (9)$$

Using that $\text{Tr}[\tilde{\sigma}_{x,z}^{\otimes m}] = \text{Tr}[\tilde{\sigma}_{x,z}]^m = 1$, for any $m \in \mathbb{N}_+$, the local-global kernel writes as

$$\begin{aligned} k_{LG}(x, z) &= \tilde{\lambda}_L \text{Tr}[\tilde{\sigma}_{x,z} |0^s\rangle \langle 0^s|] + \lambda_G \text{Tr}[\tilde{\sigma}_{x,z} |0^s\rangle \langle 0^s|]^q \\ &= \tilde{\lambda}_L \text{Tr}[(\tilde{\sigma}_{x,z} |0^s\rangle \langle 0^s|) \otimes \tilde{\sigma}_{x,z}^{\otimes q-1}] + \lambda_G \text{Tr}[(\tilde{\sigma}_{x,z} |0^s\rangle \langle 0^s|)^{\otimes q}] \\ &= \text{Tr}[\tilde{\sigma}_{x,z}^{\otimes q} O], \end{aligned} \quad (10)$$

where the measurement operator O is defined as $O = \tilde{\lambda}_L O_L + \lambda_G O_G$ with $O_L = |0^s\rangle \langle 0^s| \otimes I_s^{\otimes q-1}$ and $O_G = (|0^s\rangle \langle 0^s|)^{\otimes q}$. Using equations (9) and (10), we obtain the quantum circuit depicted in Fig. 3.

The quantum circuit implementation of the local-global kernel requires t qubits and a combination of measurement operators. Since the local-global kernel with separable global encoding can be derived from the local quantum kernel (see Equation 8), an alternative approach is to

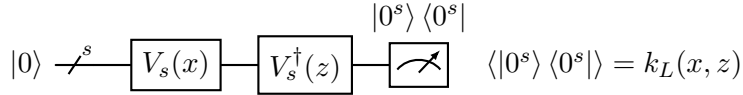


Figure 4: A quantum circuit for computing the local kernel k_L . The local-global quantum kernel $k_{LG}(x, z)$ is then obtained from k_L through classical post-processing using (8).

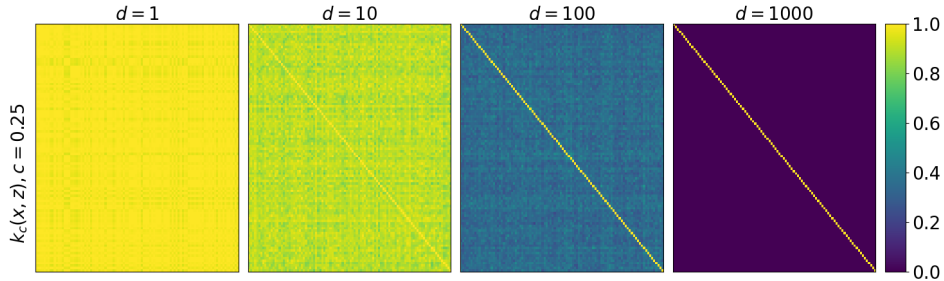


Figure 5: The kernel matrices of the quantum fidelity kernel with angle encoding are shown for different values of the dimension d , i.e., as the number of qubits increases. In angle encoding, data from $x \in \mathcal{U}([-1, 1]^d)$ is mapped to the quantum state $|\psi_x\rangle = \bigotimes_{i=1}^d R_X(cx^{(i)}) |0\rangle$, which leads to the quantum kernel $k_c(x, z) = \prod_{i=1}^d \cos^2\left(\frac{c(x^{(i)} - z^{(i)})}{2}\right)$.

use a hybrid classical-quantum scheme for its evaluation. As illustrated in Fig. 4, this scheme involves a quantum circuit that computes the local kernel, $k_L(x, z) = \text{Tr}[\tilde{\rho}_x^L \tilde{\rho}_z^L]$, followed by classical computation that computes the final kernel by raising the local kernel to the power q , as described in Equation 8. This approach is resource-efficient, as it requires only s qubits for quantum processing, with the final local-global kernel $k_{LG}(x, z)$ obtained through classical post-processing.

4 Experimental Results

In this section, we present numerical simulations demonstrating benign overfitting with local-global quantum kernels. The local-global kernel used in our experiments is defined as $k_{LG}(\mathbf{x}, \mathbf{z}) = k_c(\mathbf{x}, \mathbf{z}) + \rho k_c(\mathbf{x}, \mathbf{z})^q$, which corresponds to the kernel in (8) with $\tilde{\lambda}_L = 1$ and $\lambda_G = \rho$. We explore two approaches for constructing the local quantum kernel k_c : angle encoding [38] and Fourier representation [37].

4.1 Angle Encoding

We examine the quantum kernel defined through a feature map with a tunable bandwidth parameter c , as described in [9, 39]. This kernel is derived using a quantum angle encoding of classical data, implemented by the unitary operator given by:

$$U_c(\mathbf{x}) = \bigotimes_{j=1}^d R_X(cx_j), \text{ where } R_X(cx_j) = \begin{bmatrix} \cos\left(\frac{cx_j}{2}\right) & i \sin\left(\frac{cx_j}{2}\right) \\ i \sin\left(\frac{cx_j}{2}\right) & \cos\left(\frac{cx_j}{2}\right) \end{bmatrix}. \quad (11)$$

The resulting fidelity quantum kernel writes as [9]:

$$k_c(\mathbf{x}, \mathbf{z}) = \text{Tr}[\rho_{c,\mathbf{x}} \rho_{c,\mathbf{z}}] = \prod_{j=1}^d \cos^2\left(\frac{c(x_j - z_j)}{2}\right), \quad (12)$$

where $\rho_{c,\mathbf{x}} = U_c(\mathbf{x}) |0^d\rangle \langle 0^d| U_c^\dagger(\mathbf{x})$.

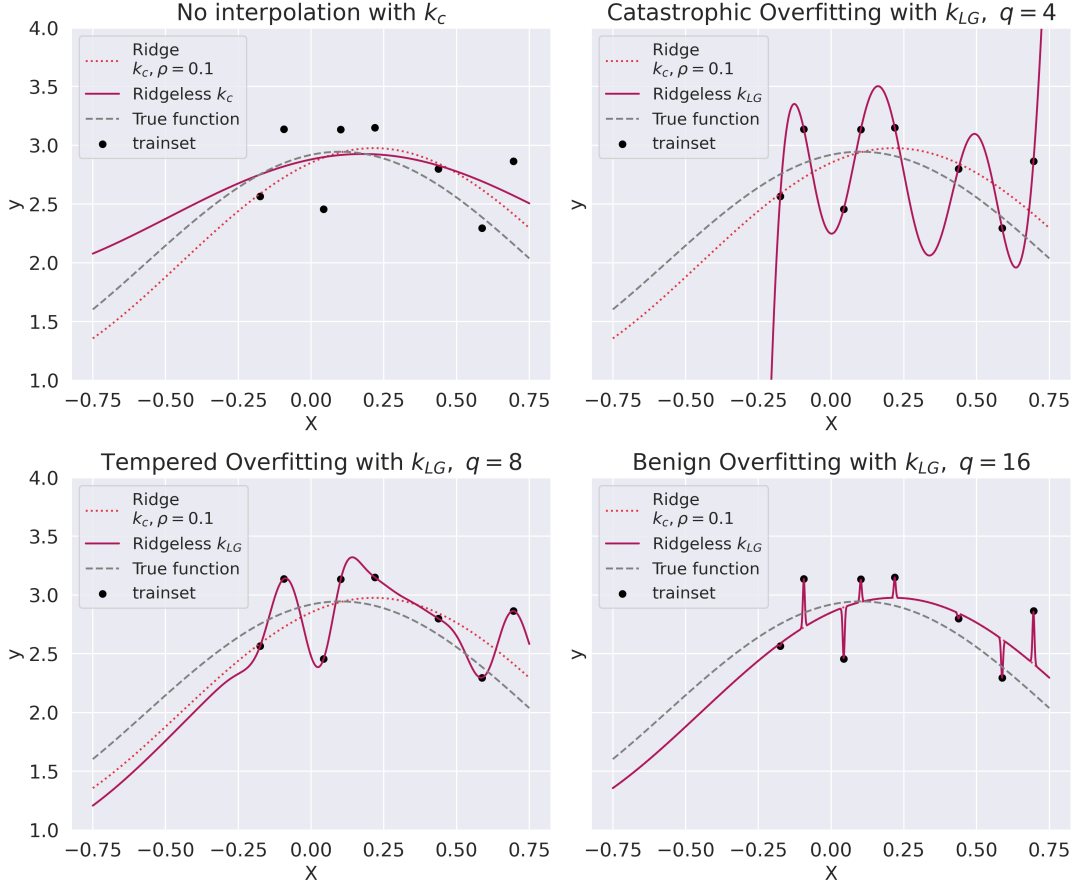


Figure 6: Overfitting behavior of local-global kernels $k_{LG}(x, z) = k_c(x, z) + \rho k_c(x, z)^q$ based on the kernel $k_c(x, z) = \cos^2\left(\frac{c(x-z)}{2}\right)$, as a function of the degree q , with $\rho = 0.1$. The local quantum kernel k_c without the global component is not expressive enough to overfit training data (upper-left). The overfitting is *catastrophic* for $q = 4$ (upper-right), *tempered* for $q = 8$ (bottom-left), and *benign* for $q = 16$ (bottom-right).

Figure 5 illustrates the difficulty of quantum fidelity kernel in generalizing. It shows the evolution of the kernel matrix for the kernel defined in (12) as the number of qubits increases. As observed, the kernel matrix approaches the identity matrix as the dimensionality grows, i.e., as the number of qubits increases. This causes poor generalization performance.

We generate $n = 8$ samples according to $y = f(x) + \epsilon$, where $\epsilon \sim \mathcal{N}(0, 0.5)$ and $x \sim \mathcal{U}([-0.75, 0.75])$. The target function f is constructed in the reproducing kernel Hilbert space (RKHS) as $f(x) = 1 + \sum_{i=1}^5 k_c(x, w_i)$, with $c = \frac{3\pi}{4}$ and the points $\{w_i\}_{i=1}^5$ independently drawn from $\mathcal{U}([-0.75, 0.75])$. Figure 6 illustrates the function learned from data by ridgeless regression using the local-global quantum kernel. The local kernel k_c , without the global component, lacks sufficient expressivity to interpolate the training data and therefore does not induce overfitting. However, incorporating the global component enables interpolation of the training set, leading to overfitting. The overfitting behavior varies with the degree q of the local-global quantum kernel: it is *catastrophic* for $q = 4$, *tempered* for $q = 8$, and *benign* for $q = 16$. Furthermore, as q increases, the ridgeless regressor based on the local-global kernel approaches the behavior of the local ρ -Ridge regressor, highlighting that the global kernel acts as an implicit regularizer for the local kernel when q is sufficiently large. This observation is consistent with the findings of [16].

We also conduct experiments with larger dimension d . Here, the data set consists of $n = 200$ iid samples $\mathbf{x}_i \sim \mathcal{U}([-1, 1]^d)$, with $d = 20$. The labels are generated via the following model

Kernel Type	ρ	q	Train MSE	Test MSE
Local (Ridge 0.07)	0.0	–	2.44e-01	0.293
Local	0.0	–	2.42e-29	40.464
Local-Global	0.07	3	1.94e-23	0.844
Local-Global	0.07	5	2.38e-26	0.396
Local-Global	0.07	7	1.09e-27	0.286

Table 1: Comparison of the performance, in terms of mean square error (MSE), of ridge and ridgeless regression with the local quantum kernel k_c against ridgeless regression using the local-global quantum kernel k_{LG} . $k_{LG}(x, z) = k_c(x, z) + \rho k_c(x, z)^q$, where $k_c(x, z) = \prod_{j=1}^d \cos^2(c(x_j - z_j)/2)$ with $c = \frac{\pi}{20}$.

$y = \sum_{j=1}^d \cos(0.01\pi x^{(j)}) + \epsilon$, where $\epsilon \sim \mathcal{N}(0, 0.5)$. Table 1 compares the performance of ridge and ridgeless regression with the local quantum kernel against ridgeless regression using the local-global quantum kernel. The results demonstrate that the local-global quantum kernel effectively addresses the generalization issue of quantum kernels, enabling benign overfitting.

4.2 Fourier representation

In addition to the angle encoding, we conduct experiments on kernel ridgeless regression using quantum fidelity kernels, through their Fourier representations [37]. We consider the following encoding,

$$S(\mathbf{x}) = \bigotimes_{j=1}^d e^{-icx_j D_s} V_s, \quad D_s = \sum_{a=0}^{2^s-1} \lambda_a |a\rangle \langle a|, \quad V_s = H^{\otimes s}. \quad (13)$$

Using this unitary map, each component \mathbf{x} is embedded separately into a quantum state of s qubits. Controlling s controls the expressivity of the kernel. The quantum kernel function is then expressed as follows [37]:

$$k_c(\mathbf{x}, \mathbf{z}) = \left| \langle 0^t | S(\mathbf{x}) S^\dagger(\mathbf{z}) | 0^t \rangle \right|^2 = \prod_{j=1}^d \frac{1}{2^{2s}} \sum_{a,b=0}^{2^s-1} e^{-ic(\lambda_a - \lambda_b)(x_j - z_j)}. \quad (14)$$

In terms of implementation, the diagonal operator $e^{-icx_j D_s}$ can be efficiently realized (see, eg. [45]), while V_s is implemented as a tensor product of Hadamard gates.

The dataset we consider consists of $n = 1000$ training samples uniformly drawn from $[-1, 1]^d$ ($d = 5$), with outputs generated as $y = \sin(\sum_{i=1}^d x_i) + \epsilon$, where $\epsilon \sim \mathcal{N}(0, 0.1)$ represents Gaussian noise. We set $\rho = 1/n$ and $c = 1$, and consider the diagonal matrix D_s defined as $D_s = \text{diag}[D_{s-1}^+, D_{s-1}^-]$, where $s = 5$, $D_{s-1}^- = -D_{s-1}^+$ and $D_{s-1}^+ = \text{diag}(\{\frac{1}{m}\}_{m=1}^{2^{s-1}})$.

Table 2 presents the mean squared error (MSE) performance of ridgeless regression using local-global quantum kernels, which are computed using the Fourier representation of quantum fidelity kernels. The results demonstrate that local-global kernels can significantly enhance the performance of quantum kernels by achieving benign overfitting.

Figure 7 displays the eigenvalues of the kernel matrix associated with the local-global quantum kernels constructed using k_c in (14). It illustrates that, for sufficiently high values of q , our local-global kernel approach results in kernel matrices of the form $K \approx K_{<l} + \rho I$, which promotes benign overfitting.

5 Conclusion

We introduced a novel approach to quantum kernel construction, called local-global kernels, which combines local and global components to enable benign overfitting in quantum machine

Kernel Type	q	Train MSE	Test MSE
Local	–	5.14e-10	2.105
Local-Global	5	6.68e-14	0.407
Local-Global	10	2.23e-17	0.133
Local-Global	50	6.60e-23	0.020
Local-Global	100	7.52e-24	0.016

Table 2: Mean square error (MSE) performance of kernel Ridgeless regression with local-global quantum kernels computed using the Fourier representation of quantum fidelity kernels (see equation 14).

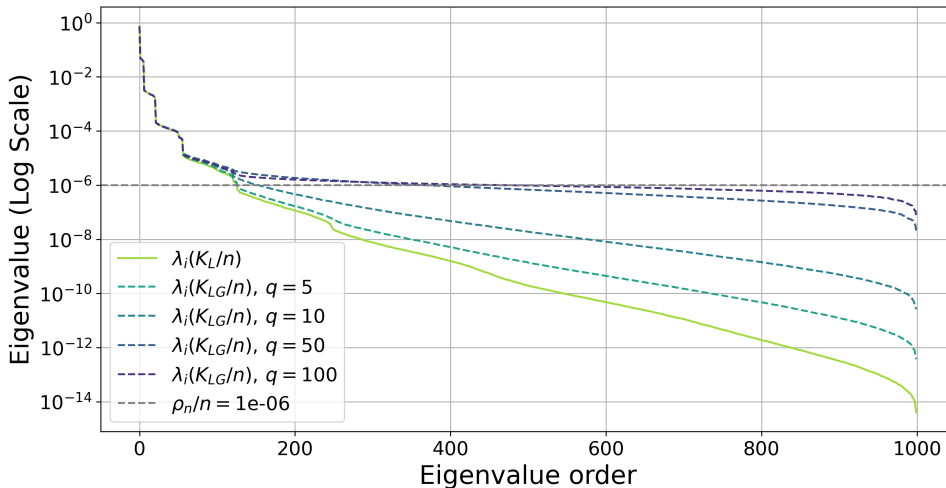


Figure 7: Eigenvalues of kernel matrices of local-global quantum kernels constructed using k_c in (14).

learning. By leveraging separable global encoding, we offer a simple mechanism to control the bandwidth of the global kernel component. Our empirical results demonstrate that adjusting the spikiness of the global component fosters benign overfitting. While this approach is designed to promote benign overfitting, it also presents a promising strategy for constructing effective quantum kernels.

Acknowledgments

H.K. is partially supported by grant ANR-19-CE23-0011 from the French National Research Agency. J.T. would like to thank Kais Hariz and Ugo Nzongani for their helpful discussions.

References

- [1] Peter L Bartlett, Philip M Long, Gábor Lugosi, and Alexander Tsigler. Benign overfitting in linear regression. *Proceedings of the National Academy of Sciences*, 2020.
- [2] Peter L Bartlett, Andrea Montanari, and Alexander Rakhlin. Deep learning: a statistical viewpoint. *Acta numerica*, 2021.
- [3] Daniel Barzilai and Ohad Shamir. Generalization in kernel regression under realistic assumptions. In *Proceedings of the 41st International Conference on Machine Learning*. PMLR, 2024.

- [4] Daniel Beaglehole, Mikhail Belkin, and Parthe Pandit. On the inconsistency of kernel ridgeless regression in fixed dimensions. *SIAM Journal on Mathematics of Data Science*, 2023.
- [5] Mikhail Belkin, Alexander Rakhlin, and Alexandre B Tsybakov. Does data interpolation contradict statistical optimality? In *The 22nd International Conference on Artificial Intelligence and Statistics*. PMLR, 2019.
- [6] Marcello Benedetti, Erika Lloyd, Stefan Sack, and Mattia Fiorentini. Parameterized quantum circuits as machine learning models. *Quantum science and technology*, 2019.
- [7] Jacob Biamonte, Peter Wittek, Nicola Pancotti, Patrick Rebentrost, Nathan Wiebe, and Seth Lloyd. Quantum machine learning. *Nature*, 2017.
- [8] Simon Buchholz. Kernel interpolation in sobolev spaces is not consistent in low dimensions. In *Conference on Learning Theory*. PMLR, 2022.
- [9] Abdulkadir Canatar, Evan Peters, Cengiz Pehlevan, Stefan M Wild, and Ruslan Shaydulin. Bandwidth enables generalization in quantum kernel models. *arXiv preprint arXiv:2206.06686*, 2022.
- [10] Marco Cerezo, Guillaume Verdon, Hsin-Yuan Huang, Lukasz Cincio, and Patrick J Coles. Challenges and opportunities in quantum machine learning. *Nature computational science*, 2022.
- [11] Tin Sum Cheng, Aurelien Lucchi, Anastasis Kratsios, and David Belius. Characterizing overfitting in kernel ridgeless regression through the eigenspectrum. In *Proceedings of the 41st International Conference on Machine Learning*. PMLR, 2024.
- [12] Carlo Ciliberto, Mark Herbster, Alessandro Davide Ialongo, Massimiliano Pontil, Andrea Rocchetto, Simone Severini, and Leonard Wossnig. Quantum machine learning: a classical perspective. *Proceedings of the Royal Society A: Mathematical, Physical and Engineering Sciences*, 2018.
- [13] Edward Farhi, Jeffrey Goldstone, and Sam Gutmann. A quantum approximate optimization algorithm. *arXiv preprint arXiv:1411.4028*, 2014.
- [14] Elies Gil-Fuster, Jens Eisert, and Carlos Bravo-Prieto. Understanding quantum machine learning also requires rethinking generalization. *Nature Communications*, 2024.
- [15] Elies Gil-Fuster, Jens Eisert, and Vedran Dunjko. On the expressivity of embedding quantum kernels. *Machine Learning: Science and Technology*, 2024.
- [16] Moritz Haas, David Holzmüller, Ulrike Luxburg, and Ingo Steinwart. Mind the spikes: Benign overfitting of kernels and neural networks in fixed dimension. *Advances in Neural Information Processing Systems*, 2024.
- [17] Trevor Hastie, Andrea Montanari, Saharon Rosset, and Ryan J Tibshirani. Surprises in high-dimensional ridgeless least squares interpolation. *Annals of statistics*, 2022.
- [18] Vojtěch Havlíček, Antonio D Córcoles, Kristan Temme, Aram W Harrow, Abhinav Kandala, Jerry M Chow, and Jay M Gambetta. Supervised learning with quantum-enhanced feature spaces. *Nature*, 2019.
- [19] Hsin-Yuan Huang, Michael Broughton, Masoud Mohseni, Ryan Babbush, Sergio Boixo, Hartmut Neven, and Jarrod R McClean. Power of data in quantum machine learning. *Nature communications*, 2021.

- [20] Sofiene Jerbi, Lukas J Fiderer, Hendrik Poulsen Nautrup, Jonas M Kübler, Hans J Briegel, and Vedran Dunjko. Quantum machine learning beyond kernel methods. *Nature Communications*, 2023.
- [21] Marie Kempkes, Aroosa Ijaz, Elies Gil-Fuster, Carlos Bravo-Prieto, Jakob Spiegelberg, Evert van Nieuwenburg, and Vedran Dunjko. Double descent in quantum machine learning. *arXiv preprint arXiv:2501.10077*, 2025.
- [22] Jonas Kübler, Simon Buchholz, and Bernhard Schölkopf. The inductive bias of quantum kernels. *Advances in Neural Information Processing Systems*, 2021.
- [23] Martin Larocca, Nathan Ju, Diego García-Martín, Patrick J Coles, and Marco Cerezo. Theory of overparametrization in quantum neural networks. *Nature Computational Science*, 2023.
- [24] Zhu Li, Weijie Su, and Dino Sejdinovic. Benign overfitting and noisy features. *arXiv preprint arXiv:2008.02901*, 2020.
- [25] Tian Liang and Alexander Rakhlin. Just interpolate: Kernel “ridgeless” regression can generalize. In *Proceedings of the 37th International Conference on Machine Learning*, 2020.
- [26] Yunchao Liu, Srinivasan Arunachalam, and Kristan Temme. A rigorous and robust quantum speed-up in supervised machine learning. *Nature Physics*, 2021.
- [27] Neil Mallinar, James Simon, Amirhesam Abedsoltan, Parthe Pandit, Misha Belkin, and Preetum Nakkiran. Benign, tempered, or catastrophic: Toward a refined taxonomy of overfitting. *Advances in Neural Information Processing Systems*, 2022.
- [28] Marko Medvedev, Gal Vardi, and Nati Srebro. Overfitting behaviour of gaussian kernel ridgeless regression: Varying bandwidth or dimensionality. *Advances in Neural Information Processing Systems*, 2024.
- [29] Riccardo Mengoni and Alessandra Di Pierro. Kernel methods in quantum machine learning. *Quantum Machine Intelligence*, 2019.
- [30] Kosuke Mitarai, Makoto Negoro, Masahiro Kitagawa, and Keisuke Fujii. Quantum circuit learning. *Physical Review A*, 2018.
- [31] Vidya Muthukumar, Kailas Vodrahalli, Vignesh Subramanian, and Anant Sahai. Harmless interpolation of noisy data in regression. *IEEE Journal on Selected Areas in Information Theory*, 2020.
- [32] Michael A. Nielsen and Isaac L. Chuang. *Quantum Computation and Quantum Information*. Cambridge University Press, 2010.
- [33] Alberto Peruzzo, Jarrod McClean, Peter Shadbolt, Man-Hong Yung, Xiao-Qi Zhou, Peter J Love, Alán Aspuru-Guzik, and Jeremy L O’Brien. A variational eigenvalue solver on a quantum processor. *Nature Communications*, 2014.
- [34] Evan Peters and Maria Schuld. Generalization despite overfitting in quantum machine learning models. *Quantum*, 2023.
- [35] John Preskill. Quantum computing in the nisq era and beyond. *Quantum*, 2018.
- [36] Bernhard Schölkopf and Alexander J Smola. *Learning with kernels: support vector machines, regularization, optimization, and beyond*. MIT press, 2002.

- [37] Maria Schuld. Supervised quantum machine learning models are kernel methods. *arXiv preprint arXiv:2101.11020*, 2021.
- [38] Maria Schuld and Nathan Killoran. Quantum machine learning in feature Hilbert spaces. *Physical review letters*, 2019.
- [39] Ruslan Shaydulin and Stefan M Wild. Importance of kernel bandwidth in quantum machine learning. *Physical Review A*, 2022.
- [40] Yudai Suzuki, Hideaki Kawaguchi, and Naoki Yamamoto. Quantum fisher kernel for mitigating the vanishing similarity issue. *Quantum Science and Technology*, 2024.
- [41] Supanut Thanasilp, Samson Wang, M Cerezo, and Zoë Holmes. Exponential concentration in quantum kernel methods. *Nature Communications*, 2024.
- [42] Alexander Tsigler and Peter L Bartlett. Benign overfitting in ridge regression. *Journal of Machine Learning Research*, 2023.
- [43] Chiyuan Zhang, Samy Bengio, Moritz Hardt, Benjamin Recht, and Oriol Vinyals. Understanding deep learning (still) requires rethinking generalization. *Communications of the ACM*, 2021.
- [44] Haobo Zhang, Weihao Lu, and Qian Lin. The phase diagram of kernel interpolation in large dimensions. *Biometrika*, 2025.
- [45] Julien Zylberman, Ugo Nzongani, Andrea Simonetto, and Fabrice Debbasch. Efficient quantum circuits for non-unitary and unitary diagonal operators with space-time-accuracy trade-offs. *ACM Transactions on Quantum Computing*, 2024.